




## Efficient Deployment of Energy Antenna for Sensor Nodes with RF Charging

Ahmet Zorlu<sup>1</sup>, Selahattin Kosunalp<sup>2</sup>, Mehmet Baris Tabakcioglu<sup>3\*</sup>

<sup>1</sup>Bursa Technical University, Electrical-Electronics Engineering Department, Bursa, TURKEY

<sup>2</sup>University of Bayburt, Department of Electrical-Electronics Engineering, Bayburt, TURKEY

Geliş / Received: 6.11.2019, Kabul / Accepted: 19.12.2019

### Abstract

A sensor node has processor, antenna, sensor and energy units. A large number of sensor nodes generates wireless sensor network (WSN). The main problem of WSN is limited-energy. A great number of MAC protocols are introduced to compensate the energy problem. In order to supply energy to sensor nodes, an external solar panel, wind turbine and energy harvester are added to the architecture of the nodes. Moreover, wireless energy transfer is used to meet the energy problem of sensor node. Position, height and operating frequency of energy antenna is so important to charge the sensor nodes efficiently. In this study, ray theoretical models are used to calculate the electric field and generate the coverage map. As the energy antenna is deployed to optimum place, charging will complete in a short time.

**Keywords:** wireless sensor networks, wireless energy transfer, electromagnetic wave propagation, coverage

### Kablosuz Şarjlı Algılayıcı Döğümler için Verimli Enerji Anten Konumlandırma

#### Öz

Bir sensör döğümü (SD) işlemci, anten, sensör ve enerji ünitelerine sahiptir. Çok fazla sayıdaki sensör döğümleri kablosuz algılayıcı ağları (KAA) oluştururlar. KAA'ların en önemli sorunu kısıtlı enerjidir. Enerji problemini azaltmak için çok sayıda ortam erişim kontrol (MAC) protokolü ileri sürüldü. Üstelik enerji ihtiyacını karşılamak için harici güneş paneli, rüzgar türbini ve enerji hasat edici sensör döğümüne eklendi. Dahası sensör döğümünün enerji ihtiyacını karşılamak için kablosuz enerji transferi kullanıldı. Enerji antenin yeri, yüksekliği ve işlem frekansı sensör döğümlerinin verimli bir şekilde şarj etmede çok önemlidir. Bu çalışmada, elektrik alan şiddetini ve kapsama alanı haritasını çıkarmak için ışın teorisi tabanlı modeller kullanılmıştır. Enerji anteni optimum bir yere yerleştirilirse, şarj işlemi en kısa sürede tamamlanacaktır.

**Anahtar Kelimeler:** kablosuz algılayıcı ağlar, kablosuz enerji transferi, elektromanyetik dalga yayılımı, kapsama Alanı.

## 1. Introduction

Sensor is the main equipment of today's technologies. One of the basic building blocks of technologies like smart city, IoT and Industry 4.0 is sensor. Sensors are intensively preferred due to their flexibility, low error rates and low costs as they detect changes in the physical environment such as temperature,

humidity, pressure and vibration (Akyildiz et al., 2002). A lot of applications are developed using different type of sensor technologies (Yalcin et al., 2013; Yalcin et al., 2014). It is very important that the data obtained by the sensors can be transmitted to a central point and analyzed. The network formed by the combination of many sensors is called

\*Corresponding Author: mehmet.tabakcioglu@btu.edu.tr

Wireless Sensor Network (WSN). WSNs are extensively used in military, environmental, health and building applications. As in any technology, there are many areas open to improvement in WSNs. The module, which consists of sensor, processor, antenna and energy unit, is called Sensor Node (SN) (Moschitta et al., 2014). Each SN in the WSN is usually powered with battery or super-capacitor. Therefore, its energy must be used very efficiently (Kosunalp, 2016). Many different MAC protocols in data link layer have been developed to ensure energy efficiency. After a period of communication, SNs are running out of energy and battery replacement is very difficult due to their location. Therefore, providing energy to SN from external sources like solar energy or wind power is another area of study.

The most common situation is that there is an obstacle between the transmitter and the receiver when transferring energy from an external source to a SN. Due to these obstacles, the transferred energy is weakened. Electric field strength and so coverage map can be generated by electromagnetic propagation models for communication systems. Uniform theory of diffraction (UTD), slope diffraction (S-UTD) and slope UTD with convex hull (S-UTD-CH) models can be used to calculate the field strength and generate the coverage map. It is worth mentioning that this paper is an extended version of our previous study (Zorlu et al., 2002). The following sections will provide the details of the model and performance results.

## 2. Propagation Models

UTD model is proposed by Kouyoumjian and Pathak (Kouyoumjian et al., 1974). If the scenario includes only single obstacle or highly varied height distributed with multiple obstacles, UTD model can be used. As the

obstacle blocks the previous obstacle's transition region, UTD model loses the accuracy of prediction. Although the elapsed time of UTD is short, its accuracy in estimating the field strength is limited (Tabakcioglu et al., 2009). In order to calculate field strength accurately, all the diffracted, reflected and direct rays should be determined and added to total field strength (Tabakcioglu et al., 2014; Tabakcioglu et al., 2016). In the small base station conditions, obstacles can be higher than the base station, in these condition UTD model cannot calculate the field strength accurately. Instead of this model, S-UTD model proposed in (Andersen et al., 1997; Rizk et al., 1998) is used in radio planning. As the obstacle number greater than 10, instead of S-UTD model S-UTD-CH proposed in (Tabakcioglu et al., 2017) model can be used with more accurate results in a shorter time. Diffracted field can be calculated (Tzaras et al., 2001) by:

$$E = \left[ E_i D(\alpha) + \frac{\partial E_i}{\partial n} d_s(\alpha) \right] A(s) e^{-jks} \quad (1)$$

Where  $E_i$  is the incident field.  $D(\alpha)$  is the amplitude diffraction coefficient,  $n$  is the normal,  $d_s$  is slope diffraction coefficient,  $A(s)$  is the spreading factor,  $k$  is the wave number and  $s$  is the propagation distance. The amplitude diffraction coefficient is expressed by:

$$D(\alpha) = \frac{-e^{-j\pi/4}}{2\sqrt{2\pi k \cos(\alpha/2)}} F[2kL \cos^2(\alpha/2)] \quad (2)$$

Where,  $\alpha$  is the diffraction angle,  $L$  is the distance parameter for amplitude diffraction coefficient.  $F$  is the transition function and  $k$  is the wave number. The slope diffraction coefficient is given by,

$$d_s(\alpha) = \frac{1}{jk} \frac{\partial D(\alpha)}{\partial \alpha} = \frac{-e^{-j\pi/4}}{\sqrt{2\pi k}} L_s \sin(\alpha/2) (1 - F[2kL\cos^2(\alpha/2)]) \quad (3)$$

Where,  $\alpha$  is the diffraction angle,  $L_s$  is the distance parameter for slope diffraction coefficient.  $F$  is the transition function and  $k$  is the wave number. The spreading factor is expressed by:

$$A(s) = \sqrt{\frac{s_0}{s(s+s_0)}} \quad (4)$$

Where,  $s_0$  and  $s$  is propagation distance the diffraction before and after, respectively.

### 3. Simulation Results

In order to supply energy to charge the battery of sensor node, wireless energy transfer can be used (Kosunalp et al., 2017). In this study, some simulation results are given to some base station location, height and operating frequency. The simulation includes 625 SNs distributed over an area of 240 m X 240 m. In the horizontal and vertical plane, the sensor nodes are located at a distance of 10 meters each starting from 0 m X 0 m. The sensor nodes are assumed to be on the ground in a flat area. In the first case, the energy antenna is 10 m in height and placed at the starting point of the area, 0 m X 0 m. At 100 MHz frequency, electric field strength calculations are performed by UTD method. The color map of the calculations is shown in Fig. 1.

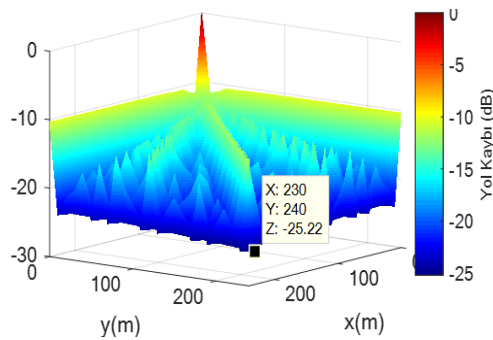


**Figure 1:** Electric field strength, transmitter height 10 m at (0,0) f=100 MHz

As seen in Fig.1, the path loss varies between -10.37 dB and -25.22 dB. In the second case, the antenna is 10 m high and placed in the middle point of the area, 120 m X 120 m. At 100 MHz frequency, electric field strength calculations are performed by UTD method. The coverage map of the scenario is illustrated in Fig. 2.

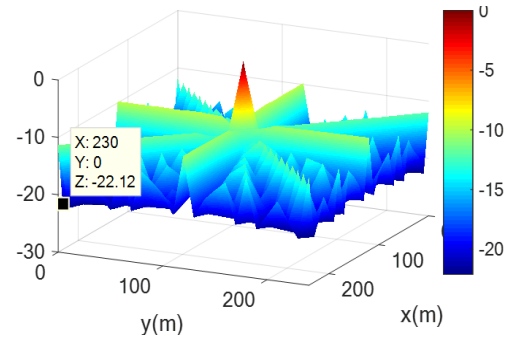


**Figure 2:** Electric field strength, transmitter height 10 m at (120,120) f=100 MHz

As it can be seen in Fig.2, the path loss varies between -9.84 dB and -22.12 dB. When the transmitter is moved from the starting point to the midpoint at 100 MHz frequency, it is seen that the electric field strength increases and the path loss decreases. In the third case, the antenna is 30 m high and placed in the middle point of the area 120 m X 120 m. At 100 MHz frequency, electric field strength calculations are performed by UTD method. The coverage map of this scenario is depicted in Fig.3.

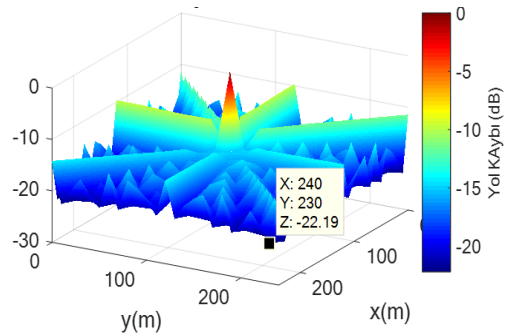


**Figure 3:** Electric field strength, transmitter height 30 m at (120,120) f=100 MHz

As it is depicted in Fig.3, the path loss varies between -9.76 dB and -22.19 dB. When the height of the transmitter is increased from 10 m to 30 m at the frequency of 100 MHz, the electric field strength decreases at all points of the transmitter and path loss increases. In the fourth case, the antenna is 10 m high and placed at 0 m X 0 m, the starting point of the area. At 2400 MHz frequency, electric field strength calculations are performed by UTD method. The coverage map of this scenario is demonstrated in Fig.4.

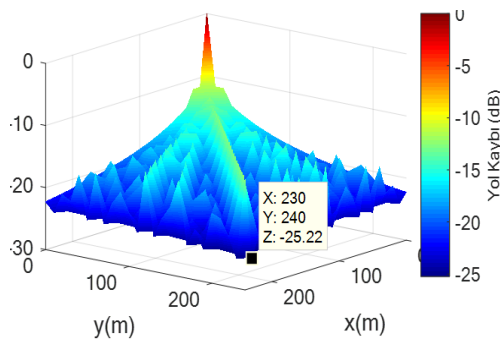


**Figure 4:** Electric field strength, transmitter height 10 m at (0,0)  $f=2400$  MHz

As it is demonstrated in Fig.4, the path loss varies between -11.51 dB and -25.22 dB. When the frequency increases from 100 MHz to 2400 MHz, it is seen that the electric field strength reaching all points decreases and path loss increases. In the fifth case, the antenna is 10 m high and located at the midpoint of the area, 120 m X 120 m. Electric field strength calculations are performed by UTD method at 2400 MHz frequency. The coverage map of this scenario is shown in Fig.5.

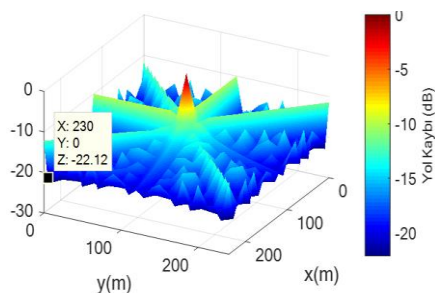


**Figure 5:** Electric field strength, transmitter height 10 m at (120,120)  $f=2400$  MHz

As shown in Fig.5, the path loss varies between -9.99 dB and -22.12 dB. When the transmitter is moved from the starting point to the midpoint at 2400 MHz, it is seen that the electric field strength increases and the path loss decreases. Similar to the condition of the transmitter at the starting point, when the frequency rises from 100 MHz to 2400 MHz, it is seen that the electric field strength reaching all points decreases and path loss increases. In the sixth case, the antenna is 30 m high and located at the midpoint of the area 120 m X 120 m. Electric field strength calculations are performed by UTD method at 2400 MHz frequency. The coverage map of this scenario is illustrated in Fig.6.

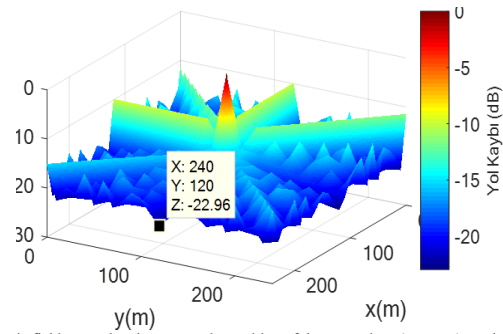


**Figure 6:** Electric field strength, transmitter height 30 m at (120,120)  $f=2400$  MHz

As it is shown in Fig.6, the path loss varies between -9.96 dB and -22.96 dB. When the height of the transmitter is increased from 10m to 30m at 2400 MHz frequency, the electric field strength decreases at all points and the path loss increases. In addition, when the frequency is increased from 100 MHz to 2400 MHz, the distance from the transmitter decreases the electric field strength and the path loss increases. According to the results obtained in the second simulation, the transmitter used as an Energy Station should be 10 m high and placed at the midpoint of the area. In this case, the highest electric field strength and the lowest path loss were observed in the receiver sensor nodes.

In the second simulation scenario optimum base station location is determined for 400 m X 400 m area. In order to generate coverage map, UTD, S-UTD and S-UTD-CH models are used. Locations of sensor nodes in x-direction is [0 20 30 60 80 120 150 180 200 225 250 300 320 350 400] and y-direction [0 20 30 60 80 120 150 180 200 225 250 300 320 350 400]. Firstly UTD model is preformed and coverage map is generated as shown in Fig. 7.

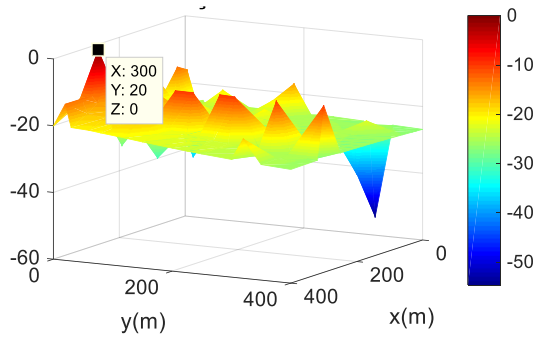


**Figure 7:** Coverage map of UTD Model.

As it is shown in Fig.7, energy antenna should be deployed in the point (300 m, 20 m). Minimum path loss value is -54.61 dB. Secondly, S-UTD model is preformed and coverage map is generated as shown in Fig. 8.

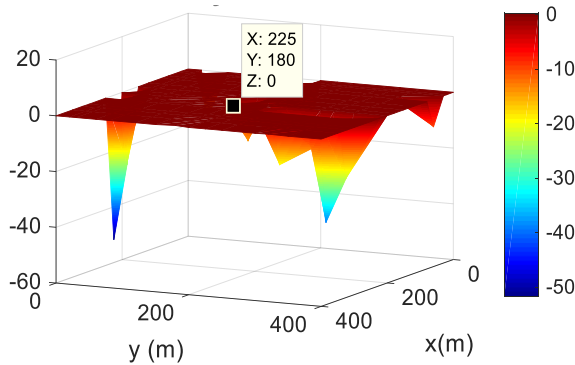


**Figure 8:** Coverage map of S-UTD Model.

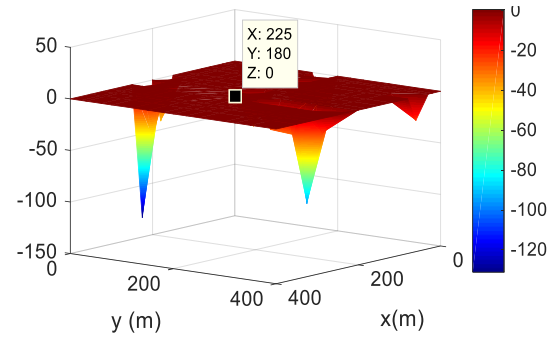


**Figure 9:** Coverage map of S-UTD-CH Model.

As it is shown in Fig.8, energy antenna should be deployed in the point (225 m, 180 m). Minimum path loss value is -51.75 dB. At third, S-UTD-CH model is preformed and coverage map is generated as shown in Fig. 9.

As it is shown in Fig.9, energy antenna should be deployed in the point (225 m, 180 m). Minimum path loss value is -131.1 dB. S-UTD-CH model gives almost the same results in shorter time.

#### 4. Conclusions

In this study, application areas and importance of WSN are mentioned. Energy consumption, which is the most important problem in WSNs, is discussed and solutions suggested. In addition to providing energy efficiency, Wireless Energy Transfer with RF from a fixed source is emphasized so that it can be supplied wirelessly with external energy sources. It has been determined that Electromagnetic Wave Propagation Models used in mobile network base station positioning can also be used in energy transmission calculations. UTD, S-UTD and S-UTD-CH models are ray tracing based electromagnetic wave propagation models. In the simulations performed by using propagation models, energy transmission tests are performed on 625 sensor nodes at the ground level by changing the position and

height of the transmitter station by changing the frequency as 100 MHz and 2400 MHz. When the transmitter is moved from the start point to the midpoint of the field at 100 MHz, the path loss is reduced and higher energy transmission to more SN is observed. When the height of the transmitter is increased from 10 m to 30 m, it is observed that the path loss increased. According to these results, the transmitter should be positioned at the optimum height for receiving SN. By increasing the frequency from 100 MHz to 2400 MHz, the electric field at all points decreases and the path loss increases.

## 5. References

- Akyildiz I.F, W. Su, Y. Sankarasubramaniam, Cayirci E. (2002). Wireless sensor networks: a survey, *Computer Networks*, (38), 393–422.
- Moschitta A., Neri I. (2014). Power consumption Assessment in Wireless Sensor Networks, <http://dx.doi.org/10.5772/57201>.
- Kosunalp, S. (2016). A Performance Evaluation of Solar Energy Prediction Approaches for Energy-Harvesting Wireless Sensor Networks, *International Journal of Applied Mathematics, Electronics and Computers*, (Issue:1), 424-427.
- Zorlu, A. Kosunalp, S. Tabakcioglu, M.B. (2019). Coverage of energy antenna radiating in different frequencies for randomly distributed sensor nodes, *3<sup>rd</sup> International Conference on Advanced Engineering Technologies*, 440-444.
- Kouyoumjian R.G., Pathak P.H. (1974). A Uniform Geometrical Theory of Diffraction for an Edge in a Perfectly Conducting Surface, *Proceedings of the IEEE*, (Volume: 62, Issue: 11), 1448-1461.
- Tabakcioglu M.B., Kara A. (2009). Comparison of Improved Slope Uniform Theory of Diffraction with Some Geometrical Optic and Physical Optic Methods for Multiple Building Diffractions, *Electromagnetics*, Cilt. 29, Sayı. 4, 303-320.
- Tabakcioglu M.B., Cansız A. (2014). Çoklu Kırınımlar İçeren Senaryolar için Elektromanyetik Dalga Yayılım Modelleri, *Uludağ Üniversitesi Mühendislik-Mimarlık Fakültesi Dergisi*, (Cilt 19, Sayı 1), 37-46.
- Tabakcioglu M.B., Çorapsız M.R. (2016). EKDZ modelinin farklı bina dağılımları içeren senaryolara uygulanarak eğim kırınımı etkisinin araştırılması, *SAÜ Fen Bil Der.* (20. Cilt, 1. Sayı), 39-45.
- Andersen J.B. (1997). UTD multiple-edge transition zone diffraction, *IEEE Transactions on Antennas And Propagation*, (vol:45,no:7) , 1093-1097.
- Rizk, K., Valenzula, R., Chiznik, D. and Gardiol, F., “Application of the slope diffraction method for urban microwave propagation prediction”, *IEEE Vehicular Tech. Conf.*, Ottawa, Canada, May 1998 Vol. 2, 1150 – 1155.
- Tabakcioglu, M.B. (2017), “A Top-down Approach to S-UTD-CH Model”, *ACES Journal*, vol. 32, no. 7, pp. 586-592.
- Tzaras, C. Saunders, S.R. (2001). An improved heuristic UTD solution for multiple- edge transition zone diffraction, *IEEE Trans. Antennas Prop.*, Cilt. 49, Sayı. 12, 1678-1682.
- Kosunalp S. Tabakcioglu, M.B. (2017). “MAC Protocols for RF Energy-Harvesting Wireless Sensor Networks: A Survey”, *International Journal of Computer Science and Information Security*, vol 15, no. 4, 28-33.
- Yalcin, O. Sayar, A. Arar, O.F. Akpınar, S. and Kosunalp. S. (2013). Approaches of Road

Boundary and Obstacle, *IFAC Proceedings Volumes*, 46(25), 211-215.

Yalcin, O. Sayar, A. Arar, O.F. Akpinar, S. and Kosunalp. S. (2014). Detection of Road Boundaries and Obstacles using LIDAR, *6<sup>th</sup> Computer Science and Electronic Engineering Conference (CEEC)*, 6-10.